Tracing prices: A flow-based cost allocation for optimized power systems

Fabian Hofmann and Alexander Kies
Frankfurt Institute for Advanced Studies (FIAS), 60438 Frankfurt, Germany

Abstract

Power system models are a valuable and widely used tool to determine cost-minimal future operation and investment under political or ecological boundary conditions. Yet they are silent about the allocation of costs of single assets, as generators or transmission lines, to consumers in the network. Existing cost-allocation methods hardly suit large networks and do not take all relevant costs into account. This paper bridges this gap. Based on Flow Tracing, it introduces the *Price Tracing* method which derives a node-to-node and from there an asset-to-consumer allocation of all costs in an optimized power system. The resulting cost allocations are transparent, plausible and in alignment with the locational marginal prices in the optimum. The approach is applied and discussed using a model of the future German power system.

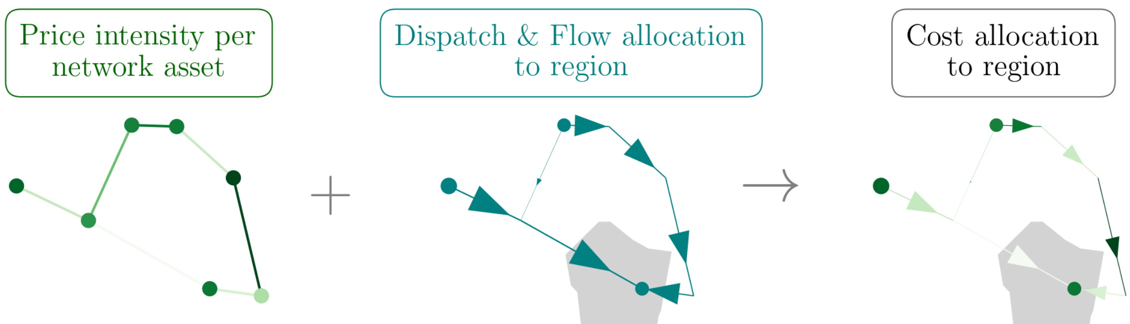

Highlights

- Cost-optimal Locational Marginal Prices are used to determine the revenues of all network assets in the system.
- Flow tracing is used to relate the revenue of each asset separately to consumers.
- This decomposes the electricity price at each node in a fair and transparent manner.
- Four use-cases are proposed and demonstrated on behalf of a future model of the German power system.

1 Introduction

Today's power systems are subject to a deep and ongoing transformation. The shift from controllable to variable, weather-driven power generation as well as the constant improvement and innovation of technology require rigorous system planning and international cooperation [1], [2]. The core of the challenge manifests in the total costs of the system. Firstly, these should be as low as possible while meeting ecological and techno-economic standards. Secondly, they must be distributed in a fair and transparent manner among all agents in the power system. It is central to identify the drivers of costs and address them appropriately. In this respect, power system models are a valuable and widely used tool [1], [3]–[5]. Many studies for countries and regions throughout the world exist that lay out how renewable energy penetration can be expanded at minimum costs. Yet they largely remain silent how and on which grounds these costs are allocated among consumers.

This paper fills this gap. We present a new method, named Price Tracing, which interlinks the electricity prices of different nodes. The method builds upon Bialek's Average Participation (AP) [6], also known as Flow Tracing, and weights the emerging power flow allocations with the Locational Marginal Price (LMP). This builds the basis for a transparent disentanglement of cost contributions to the consumer electricity prices, *i.e.* it does not only answer the question of who delivers power to whom but also how much the consumers have to pay to specific generators or transmission lines.

The literature discussed and applied the concept of flow-based cost allocation in a range of papers [7]–[13]. Shahidehpour et al. provide a profound insight into allocating congestion cost and transmission investments to market participants using different allocation techniques [8]. Specifically, they set out that Generation Shift Factors, i.e. the marginal contribution of generators to a flow on a line, allow to represent the LMP as a superposition of (a) the LMP at the reference bus, (b) the price for congestion and (c) a price for losses. The approach in [9] expands this relation for contributions based on the AP scheme, which allows for an accurate, however inexact, estimation of the optimal LMP. A similar approach on the basis of AP is used in [10] that allocates electricity prices of a non-optimal power dispatch.

In this paper, we bring together the advantages of the studies discussed above. Our approach assures cost allocations are locally constraint while fully aligning payments to the nodal pricing scheme based on the LMP. It serves to facilitate transparency and cost-benefit analysis in network plannings such as the Ten Year Network Development Plan [14] or the German Netzentwicklungsplan [15]. Further, it provides a point of departure for usage-based transmission cost allocation. While the presented method uses the Linear Optimal Power Flow (LOPF) in order to analyze large network models, we discussed how it might be extended to non-linear power flows.

At first, we formulate the Price Tracing method (section 2) with underlying assumptions and a numerical example (section 2.1). In section 3 we present possible application cases on the basis of an optimized German power system with a high share of renewable resources. Section 4 depicts methodological limitations and section 5 draws final conclusions.

2 Price Tracing

Assume an electricity network model with N nodes, L lines and T time steps. Using the linearized power flow approximation, the power flow $f_{\ell,t}$ on a passive line ℓ at time t relates to the generation $g_{n,t}$ and demand $d_{n,t}$ at node n and time t according to

$$f_{\ell,t} = \sum_n H_{\ell,n} \left(g_{n,t} - d_{n,t}\right) \quad \forall\, t \tag{1}$$

where $H_{\ell,n}$ are the Power Transfer Distribution Factors (PTDF). These translate the nodal injection on the right hand side to the network flow in compliance with the linearized Kirchhoff Circuit Laws.

In a nodal pricing scheme, the system cost occasioned by the electrical demand $d_{n,t}$ is proportional to the corresponding LMP $\lambda_{n,t}$,

$$\text{Demand Cost} : \lambda_{n,t}\, d_{n,t}. \tag{2}$$

On the other hand, system assets gain a revenue from their operation. Therefore, the revenue of the dispatch $g_{m,t}$ at bus m is given by

$$\text{Dispatch Revenue} : \lambda_{m,t}\, g_{m,t} \tag{3}$$

and the congestion revenue of line ℓ at time t by

$$\text{Congestion Revenue} : \lambda_{\ell,t}\, f_{\ell,t}. \tag{4}$$

where in the absence of network cycles the revenue per transported MWh $\lambda_{\ell,t}$ is the price difference $\lambda^{\text{diff}}_{\ell,t}$ between ending and starting node of line ℓ. In case of network cycles, the price of the Kirchhoff's Voltage Law (KVL) $\lambda^{\text{KVL}}_{\ell,t}$ may be added to $\lambda_{\ell,t}$ to adjust congestion revenues to expenditures in a long-term equilibrium, see appendices A.2 and A.4 for details. The LMP as well as the prices for the KVL are given by the dual values, often related to as shadow prices, of the corresponding constraints in the underlying cost-optimization (see appendix A.1 for details). In economic equilibrium, prices occur natrually, which in turn lead to the following equivalency

$$\underbrace{\sum_n \lambda_{n,t}\, d_{n,t}}_{\text{Total electricity cost at } t} = \underbrace{\sum_m \lambda_{m,t}\, g_{m,t} + \sum_\ell \lambda_{\ell,t} f_{\ell,t}}_{\text{Total revenue at } t} \quad \forall\, t. \tag{5}$$

While this equality relates the totals of costs and revenues, the relationships between individual contributions on the left hand side and individual contributions on the right hand side remain undefined. The following shows that by allocating flows in the network, it is possible to relate the power consumption at single nodes to the revenues of single generators and transmission lines:

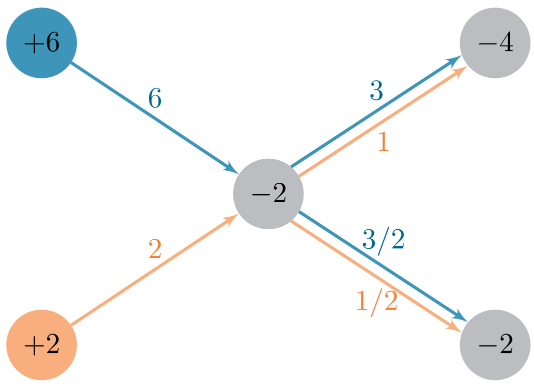

Figure 1: Schematic illustration of the AP method. Figuratively, each power source is given one color. As soon as different power flows mix at a node, the mix of “colors” in the outgoing flows are in proportion to the ingoing colors. Therefore, all consumed power can be related to a distinct origin.

Dispatch and flow can be considered as a superposition of individual contributions of nodes and assets. The literature provides various methods, called Flow Allocation (FA) method, to artificially quantify these. Each method follows a particular set of assumptions that lead to Peer-to-Peer (P2P) allocations $A_{m\to n}$ which measure the power generated at node m and consumed at node n. Flow Tracing, also known as AP [6], is a flow allocation method that traces the power injection at bus m through the network up to its sink n using the principle of proportional sharing. The method is illustrated in fig. 1 and mathematically documented in appendix B. It states that when flows from different sources meet at the same bus, their proportion determines the mix of all outgoing flows from this bus, including nodal withdrawal. The advantage of the AP method is the spatial confinement of P2P allocations $A_{m\to n}$ [16]. By definition, the sum of all recipients yields the nodal generation at m, thus

$$g_{m,t} = \sum_n A_{m\to n,t} \quad \forall\ m.t \tag{6}$$

For reasons to follow, we only resort to P2P mappings of the AP method. Thus, regardless of the AP allocation, let $A_{\ell,n,t}$ denote the contribution of demand $d_{n,t}$ to the flow on line ℓ such that the sum of all flow contributions equals flow on line ℓ,

$$f_{\ell,t} = \sum_n A_{\ell,n,t} \quad \forall\ \ell, t. \tag{7}$$

We insert eqs. (6) and (7) into eq. (5) and impose that the equality holds for all summands referring to n separately, which leads us to

$$\lambda_{n,t}\, d_{n,t} = \sum_m \lambda_{m,t} A_{m\to n,t} + \sum_\ell \lambda_{\ell,t} A_{\ell,n,t} \quad \forall\ n, t. \tag{8}$$

This equation maps the cost of nodal demand on the left-hand side to the contributions of dispatch and congestion revenues on the right-hand side. It thus indicates what consumers at n have to pay to generators at m and the transmission line ℓ. The equation introduces N new equalities for each time step of which the necessary degree of freedom comes from the yet undefined flow contribution $A_{\ell,n,t}$. In appendix A.8 we proof that

$$A_{\ell,n,t} = \sum_m H_{\ell,m}(A_{m\to n,t} - \delta_{nm} d_{n,t}) \tag{9}$$

solves eq. (8) where δ_{mn} is 1 for $m = n$ and zero otherwise. Since eq. (9) is a function of the P2P-assignment $A_{m\to n,t}$ only, the cost of electricity in eq. (8) is also only a function of the P2P allocation $A_{m\to n,t}$ and the LMP $\lambda_{n,t}$. Note that it is not possible to take the non-modified flow allocations given by the AP as these are not a solution to eq. (8). Instead we have to reassign them through eq. (9)[1].

Since generators are often grouped together at network nodes, the P2P-assignments $A_{m\to n,t}$ break down into contributions of generators located at m. Following the formulation in [17], let $A_{s,n,t} = A_{m\to n,t}\, r_{s,m,t}$ be the power allocation from generator s to demand at n where $r_{s,m,t}$ is the share that generation $g_{s,t}$ of generator s at time t contributes to the generation $g_{m,t}$ at node m and t. Naturally, it fulfills

$$g_{s,t} = \sum_n A_{s,n,t}. \tag{10}$$

Further, we set the selling price $\lambda_{s,t}$ of generator s to the LMP $\lambda_{n,t}$ with s being located at bus n. In consistency with eq. (3), the dispatch revenue of generator s is given by $\lambda_{s,t}\, g_{s,t}$.

The *Price Tracing* method for a network with a linearized power flow and a nodal pricing scheme builds

[1]This can be explained by considering that the AP flow allocations do not respect the KVL, which however have a direct effect on the LMP. For the same reason the cost estimation in [9] are inexact.

on the above equations and defines

$$\mathcal{C}_{n\to s,t} = \lambda_{s,t} A_{s,n,t} \tag{11a}$$

as the payment from consumers at n to generator s as well as

$$\mathcal{C}_{n\to \ell,t} = \lambda_{\ell,t} A_{\ell,n,t} \tag{11b}$$

as the payment to transmission line ℓ. For consistency, let $\mathcal{C}_{n,t} = \lambda_{n,t} d_{n,t}$ denote the nodal payment of all consumers at node n which according to eq. (8) is $\mathcal{C}_{n,t} = \sum_s \mathcal{C}_{n\to s,t} + \sum_\ell \mathcal{C}_{n\to\ell,t}$.

Note that storage units such as batteries may be easily introduced into the Price Tracing method: When they discharge power, they are treated like generators and when they charge power, they are treated like consumers. For the latter, the allocations $A_{s,n,t}$ and $A_{\ell,n,t}$ must be divided into allocations to consumers and charging storage units at n.

2.1 Numerical Example

In the following we illustrate the Price Tracing method in a numerical example and start with a three node network with two lines. We optimize the dispatch for one time step and perform the cost allocation. We then add a third line to the system and repeat the cost allocation to show the effect of the network cycle.

Network without Cycles

Figure 4 shows the optimized three-node network with corresponding numerical values. Both, bus 1 and 2 have a fixed demand of 30 MW and 50 MW, respectively. Bus 1 has a generator with a marginal price at 6 €/MWh. Bus 3 has a cheaper generator with marginal price at 4 €/MWh. The maximal capacity of both generators is 50 MW. The transmission line from 1 to 2 has a capacity of 60 MW and line from 3 to 1 a capacity of 30 MW. Since the latter limits the use of the cheaper generator, there is a price difference between bus 1 and 3 of 2 €/MWh. Due to the absence of network cycles, this price difference defines the congestion revenue of line 1–3. The flow on line 1–2 is not bound, hence there is no congestion revenue and bus 2 and 1 have the same electricity price of 6 €/MWh.

Since only net injections are allocated to different buses, the total demand at bus 1 is supplied by the local generator. In contrast, bus 2 imports power from bus 1 and bus 3. Using the Price Tracing method, we calculate the cost allocations $\mathcal{C}_{n\to s}$ and $\mathcal{C}_{n\to\ell}$, which we show in fig. 3. Consumers at bus 1 only have to compensate the local generator with 180 €. Consumers at bus 2 pay for congestion revenues of line 1–3, all electricity generation at bus 3 and the remaining dispatch revenues of the generator at bus 1.

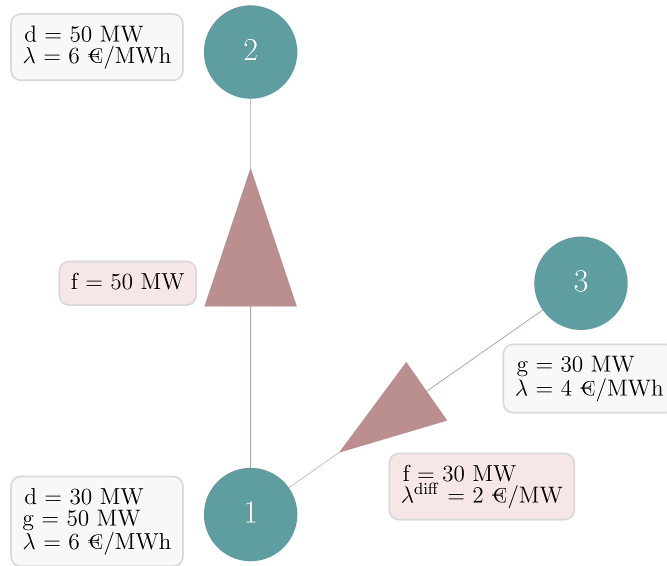

Figure 2: Example network with nodal pricing scheme. Dispatch revenue as well as demand cost per MWh are given by the LMP λ. Congestion revenue per MWh is given by the price difference λ^{diff} of the connecting nodes.

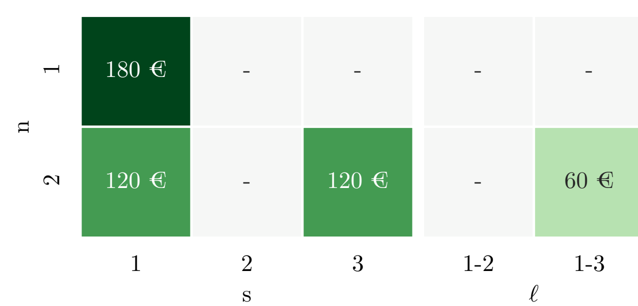

Figure 3: Allocation matrices $\mathcal{C}_{n\to s}$ (left) and $\mathcal{C}_{n\to\ell}$ (right) for the dispatch and congestion revenue for the network in fig. 2.

The consistency of the cost allocation can be easily double-checked. The sum of a column yields the payment to a generator or a line. This exactly matches the dispatch and congestion revenue defined in eqs. (3) and (4). In turn the sum of a row gives the total amount that consumers at a bus have to pay. These equal the demand cost $\lambda_n d_n$. For example the sum of payments of consumers at bus 2 is 300 € which is the price of 6 €/MWh times the consumption of 50 MWh.

Network with Cycle

Now, we add a line from bus 3 to bus 2 with a capacity of 30 MW. This introduces a KVL constraints for the three lines, requiring that the sum of flows following the cycle is zero[2]. As shown in fig. 4 the new line's capacity is bounded at 30 MW. The new cost optimum results in a higher price at bus 2 of 8 €/MWh despite that the cheaper generator 2 produces 10 MW more than before. This result may be counterintuitive, but it becomes clear when considering that the low capacity of the new line, combined with the KVL, restricts flows on line 1–3 and 1–2.

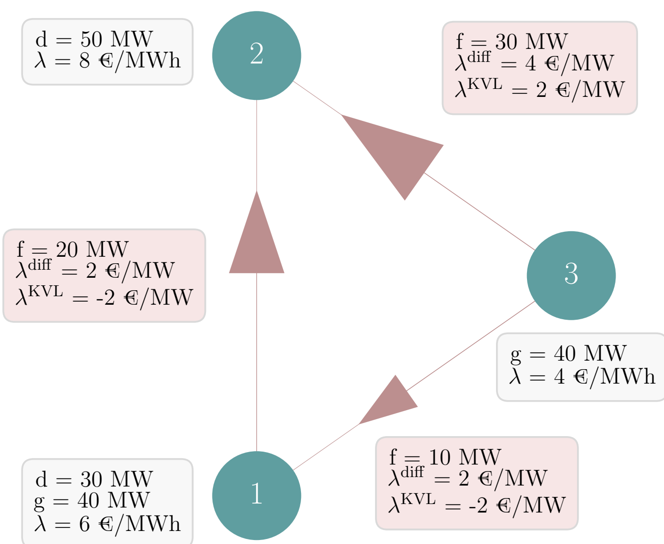

Figure 4: Example network with nodal pricing scheme and a network cycle. Now, due to the KVL a new constraint adds to the optimization problem. Optionally, the congestion revenue per MWh may include shadow prices of the KVL constraint $\lambda_{\ell,t}^{\mathrm{KVL}}$, thus $\lambda_{\ell,t} = \lambda_{\ell,t}^{\mathrm{diff}} + \lambda_{\ell,t}^{\mathrm{KVL}}$.

The prices $\lambda_{\ell}^{\mathrm{KVL}}$ of line ℓ are returned as the shadow price of the KVL constraints in the cost-optimization,

[2]For simplicity we assume a uniform impedance in the example.

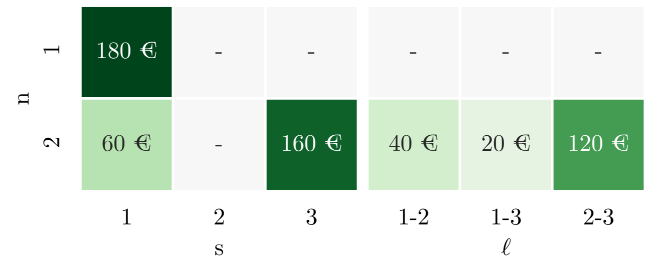

(a) Without KVL shadow prices

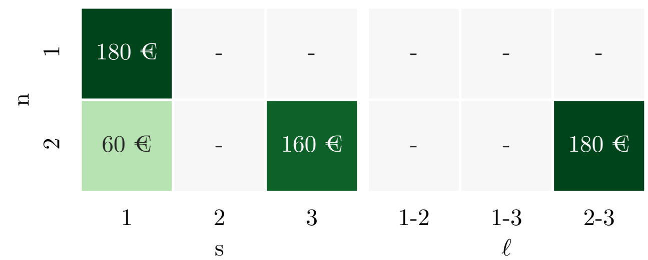

(b) With KVL shadow prices

Figure 5: Cost allocations $\mathcal{C}_{n\to s,t}$ and $\mathcal{C}_{n\to \ell,t}$ for the dispatch and congestion revenue in the network in fig. 4.

see appendix A.2 for details. The Price Tracing method optionally allows to consider these in the congestion revenue without loosing its consistency with the demand costs.

Figure 5a shows the cost allocation without considering the KVL shadow prices. Here, the congestion revenue is proportional to the price difference of the connected buses only. The new line 2–3 has the highest revenue at 120 €/MWh. In contrast fig. 5b shows the cost allocation under consideration of the KVL shadow prices. Here, the congestion revenues are shifted towards 1–2 and 1–3. Note that this shift accounts for the fact that it is the new line 2–3 that limits the flow on line 1–2 and 1–3.

Again both cost allocation schemes are consistent with the total demand cost, dispatch and congestion revenues. In the following, we consider the KVL shadow prices in the Price Tracing method since then, the total congestion revenue of a line equals the sum of all associated line costs in a short and long-term equilibrium, see appendix A.4.

3 Application Cases

Using a cost-optimized model of the German power system with 50 representative nodes and a one year

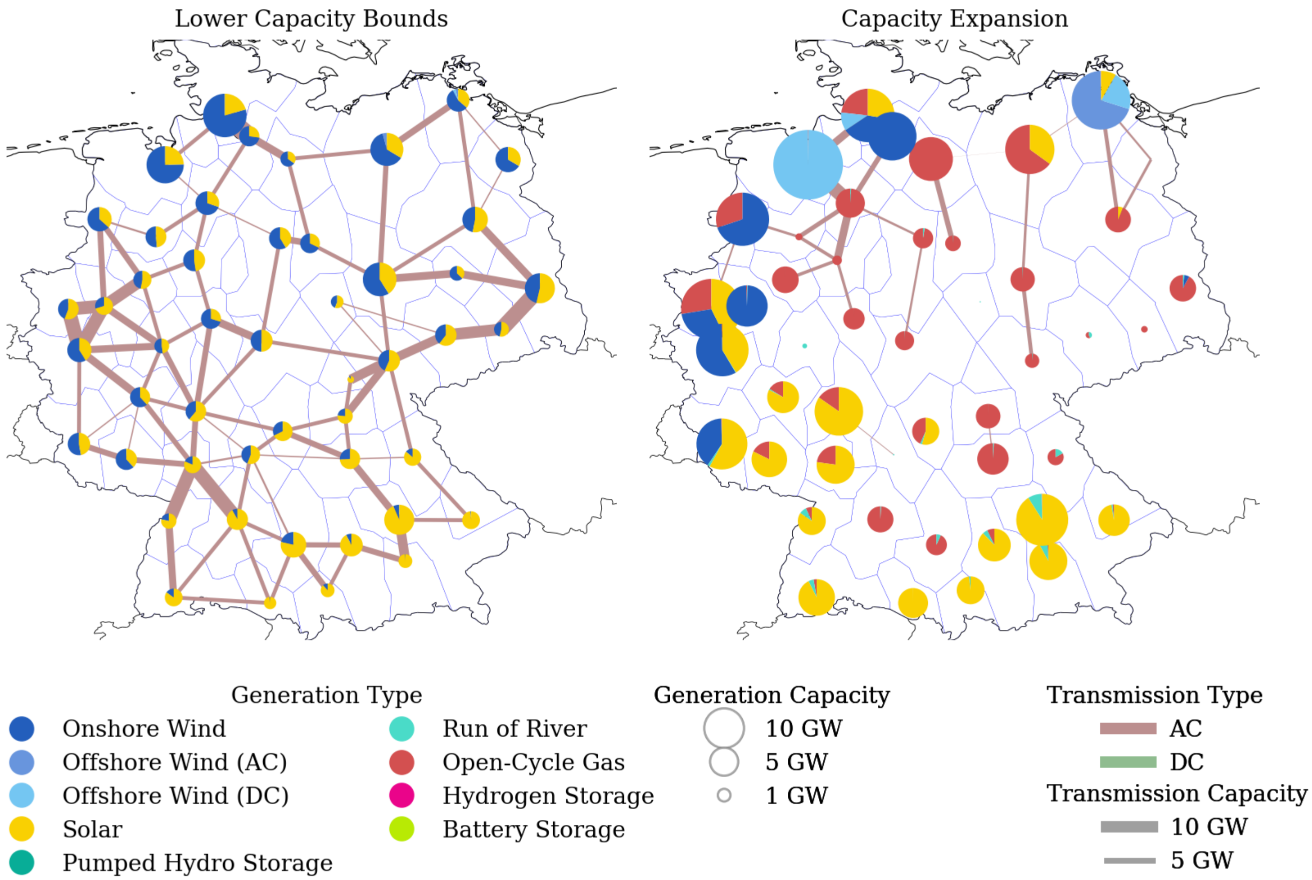

Figure 6: Model of the German power system. The left hand side shows minimum requirements for renewable and transmission capacities. The right hand side shows the cost-optimal capacities of all generators as well as transmission expansions. The effective CO_2 price is set to 120 € per tonne CO_2 emission.

time span with hourly resolution, we demonstrate four use cases of the Price Tracing method.

The investment model builds up on the PyPSA-EUR workflow [18] whose technical details and assumptions are presented in [19]. Transmission line capacities can be expanded but require a minimum of today's capacities, originally retrieved from the ENTSO-E Transmission System Map [20]. Further, we require a minimum deployment of renewable capacity derived from matching all entries of the OPSD renewable power plant list [21] to its closest bus. Wind and solar capacity expansion are limited by land-use restrictions considering agriculture, urban, forested and protected areas based on the CORINE and NATURA2000 database [22], [23]. Pumped-Hydro-Storage (PHS) and Run-of-River (ROR) power plants are fixed to today's capacities and may not be expanded. Additionally, unlimited expansion of batteries and H_2-storages and Open-Cycle Gas Turbine (OCGT) are allowed at each node. We impose a carbon price of 120 € per tonne-CO_2 which, for OCGT, adds an effective price of 55 €/MWh_{el}(assuming a gross emission of 180 kg/MWh and an efficiency of 39%). All cost assumptions on operational costs and annualized capital cost are summarized in table 3.

The network is shown in fig. 6. The left hand side shows all minimum capacity requirements, the right hand side the cost-optimal generation capacities as well as net transmission expansions. Solar capacities are expanded in the south, onshore and offshore wind in the upper north and far west. OCGT are built in the middle and north of the country. Transmission lines are amplified along the north-south axis, including a major Direct Current (DC) link, associated with the German Süd-Link, running from the coastal region to the southwest. The total annualized cost of the power system roughly sums up to 46 billion €.

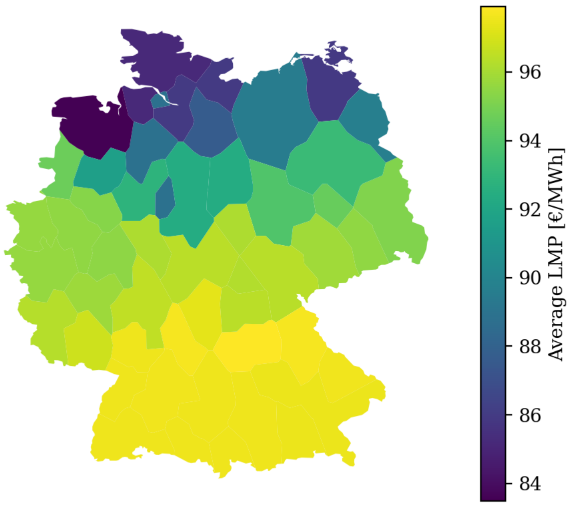

Figure 7: Load-weighted average electricity price $\bar{\lambda}_n$ per region in the optimized German power system. Regions in the middle and south of Germany have high prices whereas electricity in the North with a strong wind, transmission and OCGT infrastructure is cheaper.

Figure 7 displays the load-weighted average electricity price $\bar{\lambda}_n$ per region, defined by

$$\bar{\lambda}_n = \frac{\sum_t \lambda_{n,t} d_{n,t}}{\sum_t d_{n,t}} = \frac{\sum_t \mathcal{C}_{n,t}}{\sum_t d_{n,t}} \qquad (12)$$

It reveals a relatively strong gradient from south (at roughly 98 €/MWh) to north (84 €/MWh). Regions with little minimum capacity requirements and little capacity expansion, especially with respect to renewable generation, tend to have higher prices.

3.1 Usage-based Network Tariff

The first possible use-case of the Price Tracing method we discuss here, is a usage-based network tariff. Among other countries, electricity consumers in Germany pay a uniform network tariff, the "Netzentgelte". These are based on an relatively opaque calculation and valuation of all network cost for each Transmission System Operator, in addition to a individually derived profit margin.

The Price Tracing method allocates all congestion revenues to consumers in the network, given by $\mathcal{C}_{n\to\ell,t}$. This cost allocation can be used to define a usage-based network tariffs $\bar{\lambda}_n^{\text{grid}}$ for each bus-region n in the network:

$$\bar{\lambda}_n^{\text{grid}} = \frac{\sum_{t,\ell} \mathcal{C}_{n\to\ell,t}}{\sum_t d_{n,t}}. \qquad (13)$$

This is the average price that consumers at n pay for the transmission of electricity. These include compensations for all capital investments taken by the network operators. Consumers with a high degree of nodal autarky, *i.e.* with a little net electricity import, pay a lower network tariff and vice versa. This gives an incentive to regions with a sub-optimal deployment of renewable technologies to invest in local infrastructure. Note since the cost-optimum represents a long-term equilibrium, the total revenue per network asset equals the total Operational Expenditures (OPEX) and Capital Expenditures (CAPEX). Therefore, the network tariffs $\bar{\lambda}_n^{\text{grid}}$ do not result in any profits.

A further advantage of this network tariff allocation lays in the possibility to differentiate between different network operators. The quantity

$$\bar{\lambda}_{n\to\ell}^{\text{grid}} = \frac{\sum_t \mathcal{C}_{n\to\ell,t}}{\sum_t d_{n,t}} \qquad (14)$$

decomposes the network tariff to single lines, naturally fulfilling $\bar{\lambda}_n^{\text{grid}} = \sum_\ell \bar{\lambda}_{n\to\ell}^{\text{grid}}$. On one hand this enables to quantify operator or country specific network tariffs in consistency with cross-border flows. On the other hand this facilitates to trace back which congested lines are the strongest drivers to the local network tariff.

Figure 8 shows the network tariffs $\bar{\lambda}_n^{\text{grid}}$ for all regions of the network model as well as the average congestion revenues per transmission line. Regions close to the shore are hardly affecting the transmission system, hence their network tariff is negligible. In contrast, regions in the middle and south are relying on power transfer from the north. Their demand is the main cause for the transmission system expansion. This translates to a higher network tariff.

3.2 Emission Cost Allocation

The mapping $\mathcal{C}_{n\to s,t}$ allocates all dispatch revenues to consumers. Naturally, the revenues of conventional generators include costs accounting for CO_2 emissions. Using the mechanism of the Price Tracing method, these CO_2 costs may be mapped to consumers by weighting the dispatch allocation $A_{s,n,t}$ with the effective CO_2 price μ_{CO2} per produced MWh

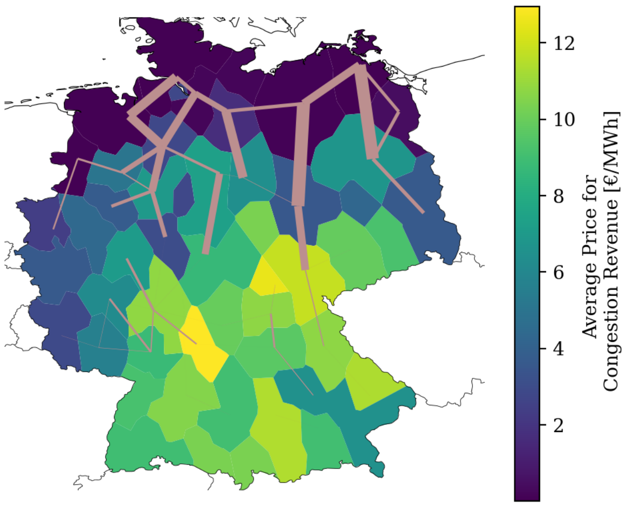

Figure 8: Usage-based network tariff per region. The resulting prices are indicated by the color of the region, the transmission lines are drawn in proportion to their congestion revenues.

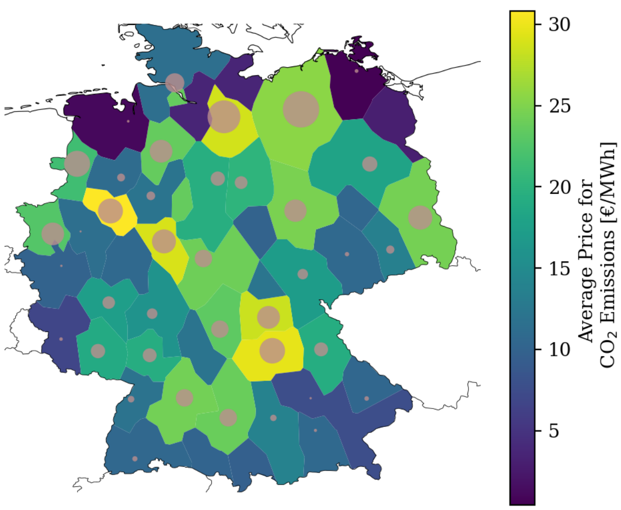

Figure 9: Average CO_2 cost per consumed MWh. The effective prices are indicated by the color of the region, the circles are drawn in proportion to the revenue per regional generators.

at generator s. Applying an emission cost allocation in the form of

$$\mathcal{E}_{n\to s,t} = \mu_{\mathrm{CO2}} A_{s,n,t} \tag{15}$$

encourage consumers to reduce their emission intensive power consumption and leads to a transparent polluter pay principle. The average emission cost per consumed MWh is then given by

$$\bar{\lambda}_n^{\mathrm{CO_2}} = \frac{\sum_{t,\ell} \mathcal{E}_{n\to s,t}}{\sum_t d_{n,t}}. \tag{16}$$

Figure 9 depicts the price for the network model. Regions with higher OCGT backup capacity tend to have higher allocated emission costs. The size of the circles is proportional to the emission cost occasioned by the local generators. Note, since the CO_2 price is given exogenously, this tracing method may also be applied to networks without a nodal pricing scheme.

3.3 A Transparent Nodal Pricing Scheme

A further application case of the Price Tracing method is to make the nodal demand cost in a network more transparent. Therefore, we are able track down which parts of the system the spent costs of consumers in a region are going to. To demonstrate this, fig. 10 shows the total P2P cost assignments $\sum_t \mathcal{C}_{n\to s,t}$ and $\sum_t \mathcal{C}_{n\to \ell,t}$ for the region with the lowest average LMP (left side) and for the region with the highest LMP (right side). The dedicated region is indicated in blue. The circles and their segments indicate the allocated dispatch revenues which are subdivided by carrier type. The lines indicate the allocated congestion revenue.

Due to its small net imports, the low-price region in the north-west is hardly charged with congestion revenues. It profits from local offshore wind farms and only a small share of the payments is allocated to remote OCGTs. In contrast, the high-priced region is highly dependent on local OCGT and the transmission system, which causes high amounts of allocated dispatch and congestion revenues. Interestingly, its payments to onshore and offshore wind infrastructure are low despite a third of its supply comes from wind power, compare fig. C.2. This leads to the conclusion, that wind power supply at this region is not restricted by exhausted wind power resources but by bottlenecks in the transmission system.

3.4 Revenue Decomposition

Finally, we demonstrate a more abstract application case of the Price Tracing method which focuses on decomposing the congestion and dispatch revenue for each asset. In a long-term equilibrium without any exogenous constraints, an network asset recovers all

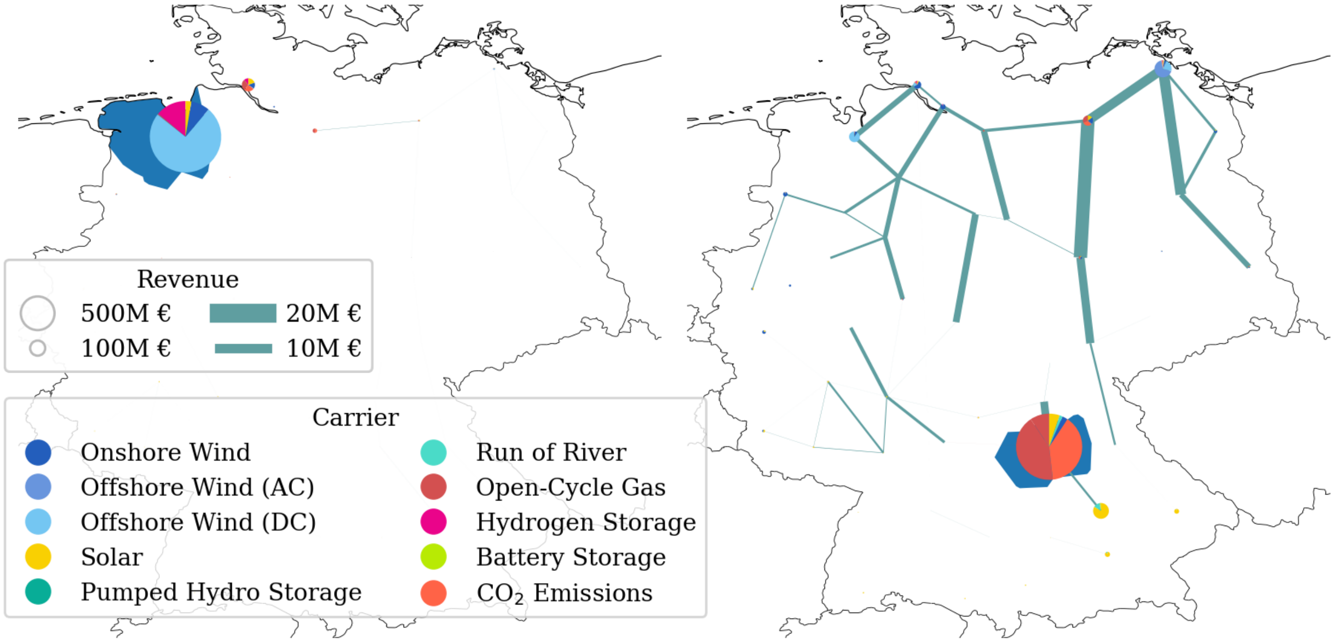

Figure 10: Comparison of payments of the region with the lowest LMP (left) and the region with the highest LMP (right). The region is colored in dark blue. The circles indicate to which bus and technology the payments are assigned. The thickness of the lines is proportional to dedicated payments.

its OPEX and CAPEX from the revenue. This relation is known as the zero-profit rule and is an outcome of the Karush–Kuhn–Tucker (KKT) conditions of the underlying cost-minimization problem, derived in detail in appendices A.3 to A.5. However, if the cost-optimum is constrained exogenously, for example by a minimum share of renewable capacity, the zero-profit relation is altered and more cost contributions have to be considered [24] as soon as the new constraint becomes binding.

Table 1: Exemplary contributions to the revenue of network assets highlighted in this work. Depending on the formulation of the optimization problem, the list changes and may possibly include other terms.

Contribution	Symbol
OPEX	$\mathcal{O}$
CAPEX	$\mathcal{I}$
Emission Tax	$\mathcal{E}$
Scarcity Rent	$\mathcal{S}$
Subsidies	$\mathcal{U}$
$\vdots$	$\vdots$

Table 1 shows a possible set of contributions to the asset revenue. On top of OPEX and CAPEX there are possible emission cost which we already discussed in section 3.2. In the presence of capacity expansion limits, additional Scarcity Rent $\mathcal{S}$ has to be considered in the revenue, in case the corresponding constraints are binding, for mathematical details see appendix A.6. This rent translates to a compensation for higher competed investments, but can also be ignored in case an asset is fixed to its existent, amortized capacity. Likewise, assets may be constrained to lower capacity requirements which reflect *i.e.* existing infrastructure known as Brownfield constraints, see appendix A.7. If binding, the lower limit reduces the revenue of the corresponding asset and leaves a Subsidy Cost $\mathcal{U}$ which have to be compensated by external institutions (government, community) or are simply ignored in case the asset is already amortized.

Except for the subsidies, all contributions can be expressed in terms of the operation of an asset, that is the generation $g_{s,t}$ and the flow $f_{\ell,t}$. Thus, given the set of discussed revenue contributions, we can decompose the dispatch revenue allocation into

$$\mathcal{C}_{n\to s,t} = \mathcal{O}_{n\to s,t} + \mathcal{I}_{n\to s,t} + \mathcal{E}_{n\to s,t} + \mathcal{S}_{n\to s,t} - \mathcal{U}_s. \tag{17}$$

where all expressions are summarized in table 2. Appendix C shows the individual cost allocations for the network model. Note that transmission lines are assumed to have neither OPEX nor emission tax, *i.e.*

$$\mathcal{C}_{n\to \ell,t} = \mathcal{I}_{n\to \ell,t} + \mathcal{S}_{n\to \ell,t} - \mathcal{U}_\ell \tag{18}$$

This approach allows modellers and system operators to disentangle the combined effect of multiple constraints on the dispatch and congestions revenue. For example, when analyzing these cost allocations for the presented German network model, it becomes clear that buses, which are far from wind farms, pay higher prices due to increased reliance in transmission and backup capacity. On the other hand, buses with high renewable installation spend most payments to local assets, see appendix C for details.

4 Limitations

The presented cost allocation is based on the linear power flow approximation. Yet, the method is equally applicable to a system with an optimal power flow, *i.e.* a Alternating Current (AC) power flow. However, in this case the allocations $A_{s,n,t}$ and $A_{\ell,n,t}$ should be computed with the Z-Bus flow allocation presented in [25] which by design respects both Kirchhoff Circuit Laws. Here, an additional cost term accounting for the transmission loss has to be considered in the decomposition of the congestion revenue.

The used optimization does not take security constrains of the transmission system into account. These may be incorporated following the approach in [11].

The method can be equally applied to short and long-term planning network models. However, the paper does not take the detailed structure of today's power markets into account. These vary form country to country and often reveal interlocked mechanisms (energy only markets, reserve markets, resdispatch etc.). The aim of the presented work is to reconsider some of the mechanisms and to reevaluate their market efficiencies.

5 Conclusion

A new method, called Price Tracing, was presented. It builds upon the nodal pricing scheme and decomposes the dispatch and congestion revenues of generators and transmission lines into individual payments of consumers. It is based on the Average Participation method which calculates assignments between generators and consumers using the principal of proportional sharing. These assignments are weighted with the market price to determine the allocation of the revenues to consumers. By means of a numerical example, we showed that there exist two options of how to treat network cycles in the cost allocation and layed out why it is more sensible to consider shadow prices of the Kirchhoff Voltage constraint.

Four application cases of the Price Tracing method were presented, using an optimized model of the German power system with a price of 120 € per tonne CO_2. Firstly, it is shown how network tariffs can be adjusted to a transparent, usage-based tariff that give incentives to invest in the local infrastructure. Secondly, the Price Tracing enables to track cost associated with CO_2 emissions through the network. This results may be used to reduce CO_2-intensive demands in a network. The third presented application case uses Price Tracing to derive cost contributions for individual consumers in order to make nodal payments transparent and explain price differences. This relates to the fourth case where individual dispatch and congestion revenues are decomposed into contributions of operational expenditure, capital expenditure, scarcity rents, subsidies. We show that the allocation can be performed for an individual cost contribution in order to give insights into power system models or to derive political advices.

Reproducibility and Expansion

All figures and data points can be reproduced by using the *python* workflow in [26]. The automated workflow allows for higher spatial resolution of the network (scalable up to a the full ENTSO-E Transmission System Map) and optionally taking the total European power system into account.

Funding

This research was funded by the by the German Federal Ministry for Economics Affairs and Energy

(BMWi) in the frame of the NetAllok project (grant number 03ET4046A) [27].

Acknowledgement

In particular, I thank Tom Brown for very fruitful discussions. I am very grateful to Alexander Zerrahn for reviewing and helping out with important parts. Further, I want to thank Alexander Kies and Markus Schlott who steadily helped with creative thoughts.

Acronyms

AC Alternating Current

AP Average Participation

CAPEX Capital Expenditures

DC Direct Current

FA Flow Allocation

KCL Kirchhoff's Current Law

KKT Karush–Kuhn–Tucker

KVL Kirchhoff's Voltage Law

LMP Locational Marginal Price

LOPF Linear Optimal Power Flow

OCGT Open-Cycle Gas Turbine

OPEX Operational Expenditures

P2P Peer-to-Peer

PHS Pumped-Hydro-Storage

PTDF Power Transfer Distribution Factors

ROR Run-of-River

A Network Optimization

A.1 Optimality Conditions

Consider the following linear minimization problem

$$\min_{x_n} \sum_n c_n \, x_n \tag{A.1}$$

subject to inequality constraints

$$g_i(x_n) \leq 0 \quad \leftrightarrow \quad \mu_i \tag{A.2}$$

and equality constraints

$$h_j(x_n) = 0 \quad \leftrightarrow \quad \lambda_j \tag{A.3}$$

where μ_i and λ_j are the corresponding dual variables, also known as KKT variables. The Lagrangian is given by

$$\mathcal{L} = \sum_n c_n x_n + \sum_i \mu_i g_i(x_n) + \sum_j \lambda_j h_j(x_n). \tag{A.4}$$

At the optimum x_n^* the following KKT conditions are satisfied.

1. Stationarity

$$\frac{\partial \mathcal{L}}{\partial x_n} = c_n + \sum_i \mu_i \frac{\partial g_i}{\partial x_n} + \sum_j \lambda_j \frac{\partial h_j}{\partial x_n} = 0 \tag{A.5}$$

2. Primal Feasibility

$$g_i(x_n) \leq 0 \qquad \forall i \tag{A.6}$$
$$h_j(x_n) \leq 0 \qquad \forall j \tag{A.7}$$

3. Dual Feasibility

$$\mu_i \geq 0 \qquad \forall i \tag{A.8}$$

4. Complementary Slackness

$$\sum_i \mu_i g_i(x_n) = 0 \tag{A.9}$$

A.2 Problem formulation

We follow a cost-minimization approach, which optimizes all operational and capital expenditures of the network. The corresponding objective is given by

$$\min_{g_{s,t}, G_s, F_{\ell,t}} \sum_{s,t} o_s g_{s,t} + \sum_s c_s G_s + \sum_\ell c_\ell F_\ell \tag{A.10}$$

where G_s and F_ℓ are the nominal capacities per generator s and line ℓ respectively. The operational costs of generators are given by o_s, the capital costs for generators and lines by c_s and c_ℓ.

Of particular importance is the nodal balance constraint which ensures that the amount of power that flows into a bus equals the power that flows out of a bus, thus reflects the Kirchhoff's Current Law (KCL). With a given demand $d_{n,t}$ this translates to

$$g_{n,t} - \sum_\ell K_{n,\ell} f_{\ell,t} = d_{n,t} \quad \leftrightarrow \quad \lambda_{n,t} \quad \forall\, n,t \tag{A.11}$$

where $K_{n,\ell}$ is +1 if line ℓ starts at bus n, -1 if it ends at n, 0 otherwise. The nodal generation $g_{n,t}$ collects the production of all nodal assets. The corresponding dual variable (or shadow price) $\lambda_{n,t}$ is the LMP per bus and time step. In an economic equilibrium for a nodal pricing scheme this is the

€/MWh$_{\mathrm{el}}$price which a consumer has to pay.

In order to impose the KVL for the linearized AC flow, the constraint

$$\sum_{\ell} C_{\ell,c}\, x_\ell\, f_{\ell,t} = 0 \quad \leftrightarrow \quad \lambda_{c,t} \quad \forall\, c, t \tag{A.12}$$

is added to the problem. Here, x_ℓ denotes the line's impedance and $C_{\ell,c}$ is $+1$ if ℓ lays aligned to the network cycle c, -1 if it lays in the opposite direction and zero if it is not part of the network cycle c. For simplicity we define the total price of the KVL per line as

$$\lambda^{\mathrm{KVL}}_{\ell,t} = \sum_{c} \lambda_{c,t}\, C_{\ell,c}\, x_\ell \quad \forall\, \ell, t. \tag{A.13}$$

The total price per transmitted unit of power can now be defined by the price differences of the starting and ending bus of the transmission line

$$\lambda_{\ell,t} = \lambda^{\mathrm{diff}}_{\ell,t} \tag{A.14}$$

with

$$\lambda^{\mathrm{diff}}_{\ell,t} = -\sum_{n} K_{n,\ell}\lambda_{n,t}. \tag{A.15}$$

or it additionally includes the price for the KVL

$$\lambda_{\ell,t} = \lambda^{\mathrm{KVL}}_{\ell,t} + \lambda^{\mathrm{diff}}_{\ell,t}. \tag{A.16}$$

A.3 Zero Profit Generation

For each generator s the optimization defines a lower and upper limit for the power output $g_{s,t}$, given by

$$-g_{s,t} \le 0 \quad \leftrightarrow \quad \underline{\mu}_{s,t} \quad \forall\, s, t \tag{A.17}$$

$$g_{s,t} - G_s \le 0 \quad \leftrightarrow \quad \bar{\mu}_{s,t} \quad \forall\, s, t \tag{A.18}$$

Constrs. (A.17) and (A.18), which yield the KKT variables $\bar{\mu}_{s,t}$ and $\underline{\mu}_{s,t}$, imply the complementary slackness,

$$\bar{\mu}_{s,t}\,(g_{s,t} - \bar{g}_{s,t}\, G_s) = 0 \quad \forall\, s, t \tag{A.19}$$

$$\underline{\mu}_{s,t}\, g_{s,t} = 0 \quad \forall\, s, t \tag{A.20}$$

The stationarity of the generation capacity variable leads to

$$\frac{\partial \mathcal{L}}{\partial G_s} = 0 \;\rightarrow\; c_s = \sum_t \bar{\mu}_{s,t}\, \bar{g}_{s,t} \quad \forall\, s \tag{A.21}$$

and the stationarity of the generation to

$$\frac{\partial \mathcal{L}}{\partial g_{s,t}} = 0 \;\rightarrow\; o_s = \sum_n K_{n,s}\, \lambda_{n,t} - \bar{\mu}_{s,t} + \underline{\mu}_{s,t} \quad \forall\, s \tag{A.22}$$

where $K_{n,s}$ is set to one if generator s is placed at node n and zero otherwise.

Multiplying both sides of eq. (A.21) with G_s and using eq. (A.19) leads to

$$c_s\, G_s = \sum_t \bar{\mu}_{s,t}\, g_{s,t} \quad \forall\, s \tag{A.23}$$

The zero-profit rule for generators is obtained by multiplying eq. (A.22) with $g_{s,t}$ and using eqs. (A.20) and (A.23) which results in

$$c_s\, G_s + \sum_t o_s g_{s,t} = \sum_{n,t} \lambda_{n,t} K_{n,s} g_{s,t} \quad \forall\, s \tag{A.24}$$

It states that over the whole time span, all OPEX and CAPEX for generator s (left hand side) are payed back by its revenue (right hand side).

A.4 Zero Profit Transmission System

For transmission lines the flow $f_{\ell,t}$ is limited by the nominal capacity F_ℓ in both directions, mathematically translating to

$$f_{\ell,t} - F_\ell \le 0 \quad \leftrightarrow \quad \bar{\mu}_{\ell,t} \quad \forall\, \ell, t \tag{A.25}$$

$$-f_{\ell,t} - F_\ell \le 0 \quad \leftrightarrow \quad \underline{\mu}_{\ell,t} \quad \forall\, \ell, t. \tag{A.26}$$

The KKT variables $\bar{\mu}_{\ell,t}$ and $\underline{\mu}_{\ell,t}$ are only non-zero if $f_{\ell,t}$ is limited by the transmission capacity in positive or negative direction, i.e. Constr. (A.25) or Constr. (A.26) are binding. For flows below the thermal limit, the complementary slackness

$$\bar{\mu}_{\ell,t}\,(f_{\ell,t} - F_\ell) = 0 \quad \forall\, \ell, t \tag{A.27}$$

$$\underline{\mu}_{\ell,t}\,(f_{\ell,t} - F_\ell) = 0 \quad \forall\, \ell, t \tag{A.28}$$

sets the respective KKT variables to zero.

The stationarity of the transmission capacity leads to

$$\frac{\partial \mathcal{L}}{\partial F_\ell} = 0 \;\rightarrow\; c_\ell = \sum_t \left(\bar{\mu}_{\ell,t} - \underline{\mu}_{\ell,t}\right) \quad \forall\, \ell \tag{A.29}$$

and the stationarity with respect to the flow to

$$0 = \frac{\partial \mathcal{L}}{\partial f_{\ell,t}} \tag{A.30}$$

$$0 = -\sum_n K_{n,\ell}\lambda_{n,t} + \sum_c \lambda_{c,t} C_{\ell,c} x_\ell - \bar{\mu}_{\ell,t} + \underline{\mu}_{\ell,t} \quad \forall\, \ell, t \tag{A.31}$$

When multiplying eq. (A.29) with F_ℓ and using the complementary slackness eqs. (A.27) and (A.28) we obtain

$$c_\ell\, F_\ell = \sum_t \left(\bar{\mu}_{\ell,t} - \underline{\mu}_{\ell,t}\right)\, f_{\ell,t} \quad \forall\, \ell \tag{A.32}$$

Again we can use this to formulate the zero-profit rule for transmission lines. We multiply eq. (A.31) with $f_{\ell,t}$, which finally leads us to

$$c_\ell\, F_\ell = -\sum_n K_{n,\ell}\, \lambda_{n,t}\, f_{\ell,t} + \sum_c \lambda_{c,t}\, C_{\ell,c}\, x_\ell\, f_{\ell,t} \quad \forall\, \ell \tag{A.33}$$

$$= \sum_t \lambda_{\ell,t} f_{\ell,t} \quad \forall\, \ell \tag{A.34}$$

where $\lambda_{\ell,t}$ is given by eq. (A.16). It states that the congestion revenue of a line (first term right hand side) reduced by the cost for cycle constraint exactly matches its CAPEX.

A.5 Zero Profit Storage Units

For an simplified storage model, the upper capacity G_r limits the discharging dispatch $g^{\mathrm{dis}}_{r,t}$, the storing power $g^{\mathrm{sto}}_{r,t}$ and state of charge $g^{\mathrm{ene}}_{r,t}$ of a storage unit r by

$$g^{\mathrm{dis}}_{r,t} - G_r \le 0 \quad \leftrightarrow \quad \bar{\mu}^{\mathrm{dis}}_{r,t} \quad \forall\, r,t \tag{A.35}$$

$$g^{\mathrm{sto}}_{r,t} - G_r \le 0 \quad \leftrightarrow \quad \bar{\mu}^{\mathrm{sto}}_{r,t} \quad \forall\, r,t \tag{A.36}$$

$$g^{\mathrm{ene}}_{r,t} - h_r\, G_r \le 0 \quad \leftrightarrow \quad \bar{\mu}^{\mathrm{ene}}_{r,t} \quad \forall\, r,t \tag{A.37}$$

where we assume a fixed ratio between dispatch and storage capacity of h_r. The state of charge must be consistent throughout every time step according to what is dispatched and stored,

$$g^{\mathrm{ene}}_{r,t} - \eta^{\mathrm{ene}}_r g^{\mathrm{ene}}_{r,t-1} - \eta^{\mathrm{sto}}_r g^{\mathrm{sto}}_{r,t} + (\eta^{\mathrm{dis}}_r)^{-1} g^{\mathrm{dis}}_{r,t} = 0 \quad \leftrightarrow \quad \lambda^{\mathrm{ene}}_{r,t} \quad \forall\, r,t \tag{A.38}$$

We use the result of Appendix B.3 in [24] which shows that a storage recovers its capital (and operational) costs from aligning dispatch and charging to the LMP, thus

$$\sum_t o_r\, g^{\mathrm{dis}}_{r,t} + c_r\, G_r = \sum_t \lambda_{n,t} K_{n,r} \left(g^{\mathrm{dis}}_{r,t} - g^{\mathrm{sto}}_{r,t}\right) \quad \forall\, r,t$$

where $K_{n,r}$ is one if storage r is paced at node n and zero otherwise. The stationarity of the dispatched power leads us to

$$\frac{\partial \mathcal{L}}{\partial g^{\mathrm{dis}}_{r,t}} = 0$$

$$o_r - \sum_n \lambda_{n,t}\, K_{n,r} - \underline{\mu}^{\mathrm{dis}}_{r,t} + \bar{\mu}^{\mathrm{dis}}_{r,t} + (\eta^{\mathrm{dis}}_r)^{-1} \lambda^{\mathrm{ene}}_{r,t} = 0 \;\forall r,t \tag{A.39}$$

which we can use to define the revenue which recovers the CAPEX at r,

$$c_r\, G_r = \sum_t \left(\bar{\mu}^{\mathrm{dis}}_{r,t} - \underline{\mu}^{\mathrm{dis}}_{r,t} + (\eta^{\mathrm{dis}}_r)^{-1} \lambda^{\mathrm{ene}}_{r,t}\right) g^{\mathrm{dis}}_{r,t} - \sum_t \lambda_{n,t} K_{n,r} g^{\mathrm{sto}}_{r,t} \quad \forall\, r \tag{A.40}$$

It stands to reason to assume that when a storage charges power, it does not supply any demand. Thus consumers only pay storage units in times the storage dispatches power. Hence, we restrict the allocatable revenue per storage unit to the first term in eq. (A.40). This allocates the CAPEX of r plus the costs $\mathcal{R}^E_r$ it needs to buy the charging power,

$$\mathcal{I}^E_r + \mathcal{R}^E_r = \sum_t \left(\bar{\mu}^{\mathrm{dis}}_{r,t} - \underline{\mu}^{\mathrm{dis}}_{r,t} + (\eta^{\mathrm{dis}}_r)^{-1} \lambda^{\mathrm{ene}}_{r,t}\right) g^{\mathrm{dis}}_{r,t} \tag{A.41}$$

In charging times the total of remaining costs $\mathcal{R}^E_r$ is spent to power from other assets. These costs scale with the amount of installed storage capacity.

A.6 Upper Capacity Expansion Limits

In real-world setups the capacity expansion of generators, lines or other assets are often limited. This might be due to land use restrictions or social acceptance considerations. When constraining the capacity S_i of an arbitrary asset i (i may now be any generator, line etc.) to an upper limit $\bar{S}$, in the form of

$$S_i - \bar{S} \le 0 \quad \leftrightarrow \quad \bar{\mu}^{\mathrm{nom}}_i, \tag{A.42a}$$

the zero profit condition alters as soon as the constraint becomes binding. Then, asset i is payed an additional scarcity rent

$$\mathcal{S}_i = -\bar{\mu}^{\mathrm{nom}}_i S_i \quad \forall\, i \in I \tag{A.42b}$$

This rent may account for different possible realms, as for example the increased market price in higher competed areas or additional costs for social or environmental compensation. The share in $\mathcal{C}_{n\to i,t}$ which consumers pay for the scarcity rent can be recalculated by a correct weighting of the shadow price $\bar{\mu}_s^{\text{nom}}$ with the capital price c_i, leading to

$$\mathcal{S}_{n\to s,t} = \frac{\bar{\mu}_i^{\text{nom}}}{c_i + \bar{\mu}_i^{\text{nom}}} \mathcal{C}_{n\to i,t} \quad \forall\, i \tag{A.42c}$$

A.7 Lower Capacity Expansion Limits

In order to take already built infrastructure into account, the capacity S_i of an arbitrary asset i may be constrained by a minimum required capacity $\underline{S}_i$. This introduces a constraint of the form

$$\underline{S} - S_i \le 0 \quad \leftrightarrow \quad \underline{\mu}_i^{\text{nom}} \tag{A.43a}$$

Again, such a setup alters the zero profit condition of asset i, as soon as the constraint becomes binding. In that case, asset i does not collect enough revenue from $\mathcal{C}_{n\to i,t}$ in order to compensate the CAPEX. The difference, given by

$$\mathcal{U}_i = \underline{\mu}_i^{\text{nom}} S_i \quad \forall\, i \tag{A.43b}$$

has to be subsidized by governments or communities or is simply ignored when investments are amortized. Allocating these cost contribution is ambiguous these as assets may not gain any revenue for their operational state.

A.8 Proof: Equivalence of local and imported prices

When inserting

$$A_{\ell,n,t} = \sum_m H_{\ell,m}(A_{m\to n,t} - \delta_{nm} d_{n,t}) \tag{A.44}$$

into

$$\lambda_{n,t}\, d_{n,t} = \sum_m \lambda_{m,t} A_{m\to n,t} + \sum_\ell \lambda_{\ell,t} A_{\ell,n,t} \quad \forall\, n,t \tag{A.45}$$

where

$$\lambda_{\ell,t} = -\sum_m K_{m,\ell}\lambda_{m,t} + \sum_c \lambda_{c,t} C_{\ell,c} x_\ell \tag{A.46}$$

the second expression on the right hand side of eq. (A.45) becomes

$$\begin{aligned}
& - \sum_{\ell,m'} H_{\ell,m'} \left(A_{m'\to n,t} - \delta_{nm'} d_{n,t}\right) \sum_m K_{m,\ell}\lambda_{m,t} \\
& + \sum_{\ell,m'} H_{\ell,m'} \left(A_{m'\to n,t} - \delta_{nm'} d_{n,t}\right) \sum_c \lambda_{c,t} C_{\ell,c} x_\ell \\
= & - \sum_{\ell,m',m} H_{\ell,m'} \left(A_{m'\to n,t} - \delta_{nm'} d_{n,t}\right) K_{m,\ell}\lambda_{m,t} \\
= & - \sum_{m',m} \delta_{mm'} \left(A_{m'\to n,t} - \delta_{nm'} d_{n,t}\right) \lambda_{m,t} \\
= & - \sum_m \left(A_{m\to n,t} - \delta_{nm} d_{n,t}\right) \lambda_{m,t} \\
= & - \sum_m A_{m\to n,t}\lambda_{m,t} + d_{n,t}\lambda_{n,t}
\end{aligned} \tag{A.47}$$

where in the third step we used the relation $\sum_\ell H_{\ell,n} K_{m,\ell} = \delta_{nm}$. The second term in the first line vanishes as the basis cycles $C_{\ell,c}$ are the kernel of the PTDF, $\sum_\ell C_{\ell,c} H_{\ell,n} = 0\ \forall c, n$.

B Power Allocation

Allocating net injections using the AP method is derived from [28]. In a lossless network the downstream and upstream formulations result in the same P2P allocation which is why we restrict ourselves to the downstream formulation only. In a first step we define a time-dependent auxiliary matrix $\mathcal{J}_t$ which is the inverse of the $N \times N$ with directed power flow $m \to n$ at entry (m,n) for $m \ne n$ and the total flow passing node m at entry (m,m) at time step t. Mathematically this translates to

$$\mathcal{J}_t = \left(\text{diag}\left(p^+\right) + \mathcal{K}^- \,\text{diag}\left(f\right)\; K\right)_t^{-1} \tag{B.48}$$

where $\mathcal{K}^-$ is the negative part of the directed Incidence matrix $\mathcal{K}_{n,\ell} = \text{sign}\left(f_\ell\right) K_{n,\ell}$. Then the P2P allocation for time step t is given by

$$A_{m\to n,t} = \mathcal{J}_{m,n,t}\, p^+_{m,t}\, p^-_{n,t} \tag{B.49}$$

	Symbol	Total Cost	Allocation
OPEX Production	$\mathcal{O}^G$	$\sum_t o_s\, g_{s,t}$	$o_s A_{s,n,t}$
OPEX Storage	$\mathcal{O}^E$	$\sum_t o_r\, g_{r,t}^{\text{dis}}$	$o_r A_{r,n,t}$
Emission Cost	$\mathcal{E}$	$\mu_{\text{CO2}}\, e_s\, g_{s,t}$	$\mu_{\text{CO2}}\, e_s A_{s,n,t}$
CAPEX Production	$\mathcal{I}^G$	$c_s G_s$	$\bar{\mu}_{s,t} A_{s,n,t}$
CAPEX Transmission	$\mathcal{I}^F$	$c_\ell F_\ell$	$\left(\bar{\mu}_{\ell,t} \underline{\mu}_{\ell,t}\right) A_{\ell,n,t}$
CAPEX Storage	$\mathcal{I}^E$	$c_r G_r$	$\left(\bar{\mu}^{\text{dis}}_{r,t} \underline{\mu}^{\text{dis}}_{r,t} + (\eta^{\text{dis}}_r)^1 \lambda^{\text{ene}}_{r,t}\right) A_{r,n,t}$

Table 2: Different cost terms and cost allocations of different assets, index s refers to generators, ℓ to lines and r to storage units. The definition of the cost weightings are defined in appendices A.3 to A.5.

C Application Case

The following figures contain more detailed information about the peer-to-peer cost allocation discussed in section 3. The cost or prices payed by consumers are indicated by the region color. The dedicated revenue is displayed in proportion to the size of cycles (for assets attached to buses) or to the thickness of transmission branches.

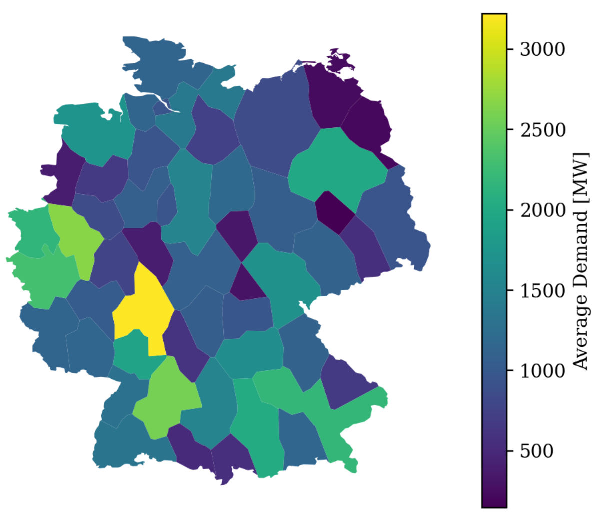

Figure C.1: Average demand, $\sum_t d_{n,t}/T$ per regions. The regions with high population densities and larger areas reveal a higher demand.

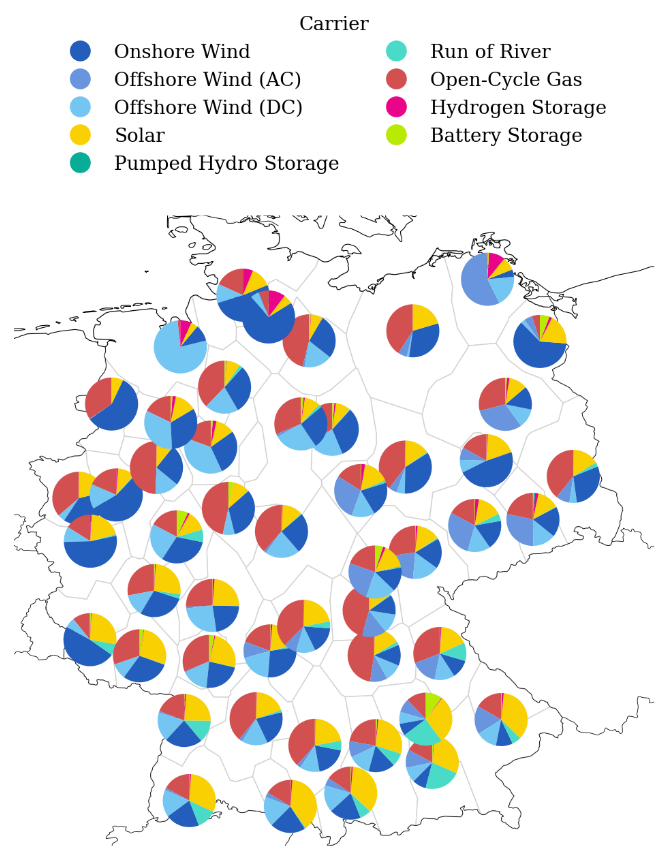

Figure C.2: Average power mix per region calculated by Average Participation. Coastal regions are mainly supplied by local offshore and onshore wind farms. Their strong power injections additionally penetrate the network up to the southern border. In the middle and South, the supply is dominated by a combination of OCGT and solar power.

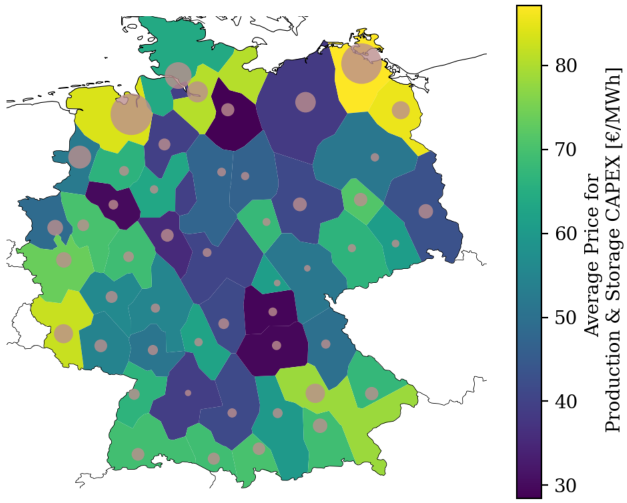

(a) All production and storage technologies

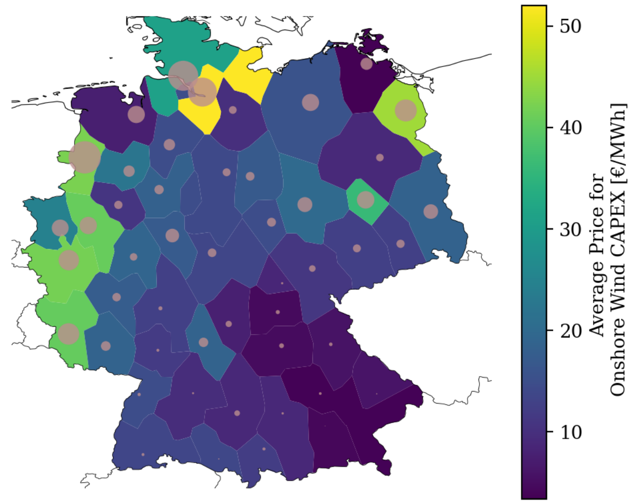

(b) Onshore Wind

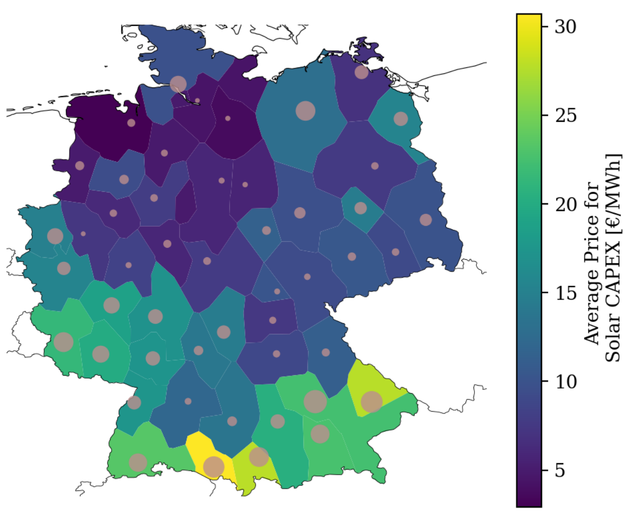

(c) Solar

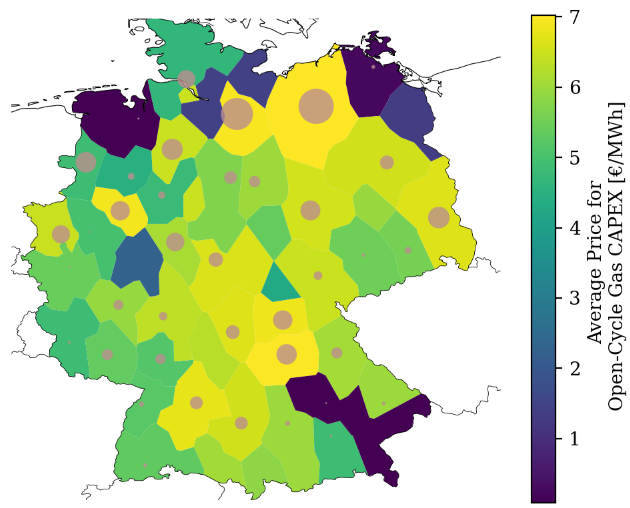

(d) OCGT

Figure C.3: Average CAPEX allocation per MWh, $\sum_t \mathcal{I}_{n\to s,t} / \sum_t d_{n,t}$ for all production and storage assets (a), onshore wind (b), solar (c) and OCGT (d). Average allocated CAPEX per MWh within the regions are indicated by the color, the revenue per production asset is given by the size of the circles at the corresponding bus.

	carrier	o [€/MWh]	c [k€/MW]*
Generator	Open-Cycle Gas	130.308	47.235
	Offshore Wind (AC)	0.015	204.179
	Offshore Wind (DC)	0.015	230.093
	Onshore Wind	0.015	109.296
	Run of River		270.941
	Solar	0.01	55.064
Storage	Hydrogen Storage		224.739
	Pumped Hydro Storage		160.627
	Battery Storage		133.775
Line	AC		0.038
	DC		0.070

Table 3: Operational and capital price assumptions for all type of assets used in the working example. The capital price for transmission lines are given in [k€/MW/km]. The cost assumptions are retrieved from the PyPSA-EUR model [18].

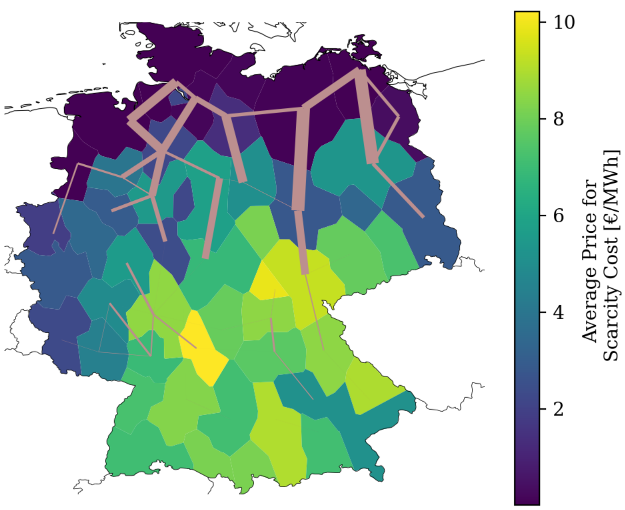

Figure C.4: Average allocated transmission scarcity cost per consumed MWh, $\sum_t \mathcal{S}_{n\to\ell,t} / \sum_t d_{n,t}$. This scarcity cost results from the upper transmission expansion limit of 25%. The costs are indicated by the regional color. The lines are drawn in proportion to revenue dedicated to scarcity cost.

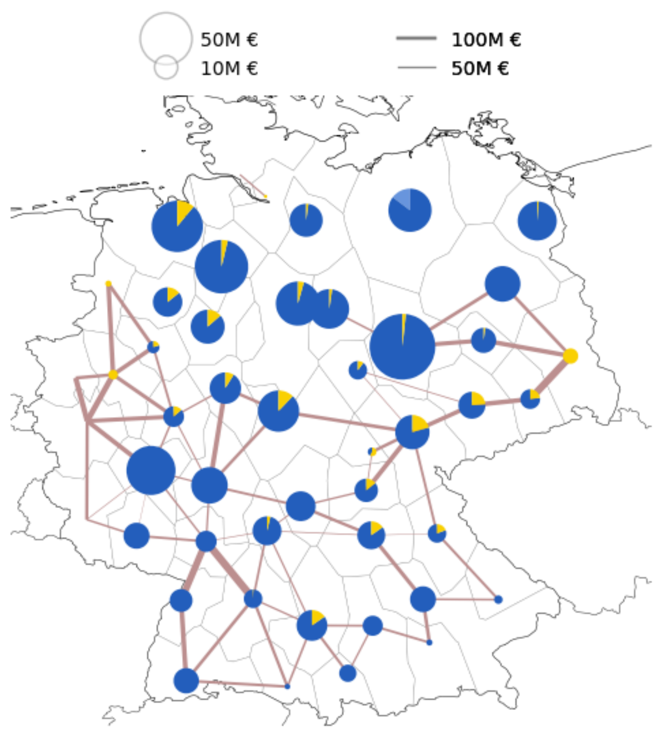

Figure C.5: Total costs for subsidy $\mathcal{U}$ resulting from lower capacity expansion bounds (brownfield constraints). The figure shows the built infrastructure that does not gain back its CAPEX from its market revenue, but is only built due to lower capacity limits.

References

[1] S. Pfenninger, A. Hawkes, and J. Keirstead, "Energy systems modeling for twenty-first century energy challenges," en, *Renewable and Sustainable Energy Reviews*, vol. 33, pp. 74–86, May 2014, ISSN: 13640321. DOI: 10.1016/j.rser.2014.02.003.

[2] D. Schlachtberger, T. Brown, S. Schramm, and M. Greiner, "The benefits of cooperation in a highly renewable European electricity network," en, *Energy*, vol. 134, pp. 469–481, Sep. 2017, ISSN: 03605442. DOI: 10.1016/j.energy.2017.06.004.

[3] A. A. Bazmi and G. Zahedi, "Sustainable energy systems: Role of optimization modeling techniques in power generation and supply—A review," en, *Renewable and Sustainable Energy Reviews*, vol. 15, no. 8, pp. 3480–3500, Oct. 2011, ISSN: 13640321. DOI: 10.1016/j.rser.2011.05.003.

[4] S. Pereira, P. Ferreira, and A. Vaz, "Generation expansion planning with high share of renewables of variable output," en, *Applied Energy*, vol. 190, pp. 1275–1288, Mar. 2017, ISSN: 03062619. DOI: 10.1016/j.apenergy.2017.01.025.

[5] T. Brown, M. Schäfer, and M. Greiner, "Sectoral Interactions as Carbon Dioxide Emissions Approach Zero in a Highly-Renewable European Energy System," en, *Energies*, vol. 12, no. 6, p. 1032, Mar. 2019, ISSN: 1996-1073. DOI: 10.3390/en12061032.

[6] J. Bialek, "Tracing the flow of electricity," en, *IEE Proceedings - Generation, Transmission and Distribution*, vol. 143, no. 4, p. 313, 1996, ISSN: 13502360. DOI: 10.1049/ip-gtd:19960461.

[7] F. Galiana, A. Conejo, and H. Gil, "Transmission network cost allocation based on equivalent bilateral exchanges," en, *IEEE Transactions on Power Systems*, vol. 18, no. 4, pp. 1425–1431, Nov. 2003, ISSN: 0885-8950. DOI: 10.1109/TPWRS.2003.818689.

[8] M. Shahidehpour, H. Yamin, and Z. Li, *Market Operations in Electric Power Systems*, en. New York, USA: John Wiley & Sons, Inc., Apr. 2002, ISBN: 978-0-471-44337-7 978-0-471-22412-9. DOI: 10.1002/047122412X.

[9] Y. Meng and B. Jeyasurya, "Investigation of Transmission Cost Allocation Using a Power Flow Tracing Method," in *2007 IEEE Power Engineering Society General Meeting*, Tampa, FL, USA: IEEE, Jun. 2007, pp. 1–7, ISBN: 978-1-4244-1296-9 978-1-4244-1298-3. DOI: 10.1109/PES.2007.385565.

[10] M. Schäfer, L. Schwenk-Nebbe, J. Hörsch, B. Tranberg, and M. Greiner, "Allocation of nodal costs in heterogeneous highly renewable European electricity networks," in *2017 14th International Conference on the European Energy Market (EEM)*, Dresden, Germany: IEEE, Jun. 2017, pp. 1–6, ISBN: 978-1-5090-5499-2. DOI: 10.1109/EEM.2017.7981964.

[11] J. Nikoukar and M. R. Haghifam, "Transmission pricing and recovery of investment costs in the deregulated power system based on optimal circuit prices," en, *Journal of Zhejiang University SCIENCE C*, vol. 13, no. 1, pp. 48–57, Jan. 2012, ISSN: 1869-1951, 1869-196X. DOI: 10.1631/jzus.C1100076.

[12] A. Arabali, S. H. Hosseini, and M. Moeini-Aghtaie, "Pricing of transmission services: An efficient analysis based on fixed and variable imposed costs," in *2012 11th International Conference on Environment and Electrical Engineering*, Venice, Italy: IEEE, May 2012, pp. 407–412, ISBN: 978-1-4577-1829-8 978-1-4577-1830-4 978-1-4577-1828-1. DOI: 10.1109/EEEIC.2012.6221412.

[13] T. Wu, Z. Alaywan, and A. Papalexopoulos, "Locational Marginal Price Calculations Using the Distributed-Slack Power-Flow Formulation," en, *IEEE Transactions on Power Systems*, vol. 20, no. 2, pp. 1188–1190, May 2005, ISSN: 0885-8950. DOI: 10.1109/TPWRS.2005.846156.

[14] ENTSO-E, "Completing the map – Power system needs in 2030 and 2040," en, p. 70, 2020.

[15] Bundesnetzagentur, *Netzentwicklungsplan Strom — Netzentwicklungsplan*, https://www.netzentwicklungsplan.de/de, 2020.

[16] F. Hofmann, A. Zerrahn, and C. Gaete-Morales, "Techno-economic criteria to evaluate power flow allocation schemes," *arXiv:2010.11000 [physics]*, Oct. 2020. arXiv: 2010.11000 [physics].

[17] M. Schafer, B. Tranberg, D. Jones, and A. Weidlich, "Tracing carbon dioxide emissions in the European electricity markets," in *2020 17th International Conference on the European Energy Market (EEM)*, Stockholm, Sweden: IEEE, Sep. 2020, pp. 1–6, ISBN: 978-1-72816-919-4. DOI: 10.1109/EEM49802.2020.9221928.

[18] J. Hörsch, F. Neumann, F. Hofmann, D. Schlachtberger, and T. Brown, *PyPSA-Eur: An Open Optimisation Model of the European Transmission System (Code)*, Zenodo, Jun. 2020. DOI: 10.5281/ZENODO.3520874.

[19] J. Hörsch, F. Hofmann, D. Schlachtberger, and T. Brown, "PyPSA-Eur: An open optimisation model of the European transmission system," en, *Energy Strategy Reviews*, vol. 22, pp. 207–215, Nov. 2018, ISSN: 2211467X. DOI: 10.1016/j.esr.2018.08.012.

[20] ENTSO-E, *ENTSO-E Transmission System Map*, en-us, https://www.entsoe.eu/data/map/.

[21] I. Schlecht and M. Simic, *Renewable power plants*, Aug. 2020. DOI: 10.25832/RENEWABLE_POWER_PLANTS/2020-08-25.

[22] EEA, "Corine Land Cover (CLC) 2012, version 18.5.1," 2012.

[23] ——, "Natura 2000 data - the European network of protected sites," 2016.

[24] T. Brown and L. Reichenberg, "Decreasing market value of variable renewables is a result of policy, not variability," *arXiv:2002.05209 [econ, math, q-fin]*, Feb. 2020. arXiv: 2002.05209 [econ, math, q-fin].

[25] A. J. Conejo, J. Contreras, D. A. Lima, and A. Padilha-Feltrin, "Z-bus Transmission Network Cost Allocation," en, *IEEE Transactions on Power Systems*, vol. 22, no. 1, pp. 342–349, Feb. 2007, ISSN: 0885-8950. DOI: 10.1109/TPWRS.2006.889138.

[26] F. Hofmann, *Pypsa-costallocation*, en, https://github.com/FabianHofmann/pypsa-costallocation, 2020.

[27] Bundesministerium für Wirtschaft und Energie, *Verbundvorhaben: NET-ALLOK - Methoden und Anwendungen der Netzkostenallokation, Teilvorhaben: Methoden und Analyse von Kostenallokationsmethoden im Betrieb des Elektrizitätssystems*, https://www.enargus.de/pub/bscw.cgi/?op=enargus.eps2 allok&v=10&id=399670.

[28] C. Achayuthakan, C. J. Dent, J. W. Bialek, and W. Ongsakul, "Electricity Tracing in Systems With and Without Circulating Flows: Physical Insights and Mathematical Proofs," en, *IEEE Transactions on Power Systems*, vol. 25, no. 2, pp. 1078–1087, May 2010, ISSN: 0885-8950, 1558-0679. DOI: 10.1109/TPWRS.2009.2037506.